Ultralow-power all-optical switching

Marin Soljačić,[a] Elefterios Lidorikis, and J. D. Joannopoulos
Department of Physics, Massachusetts Institute of Technology, Cambridge, Massachusetts 02139

Lene Vestergaard Hau
Lyman Laboratory, Harvard University, Cambridge, Massachusetts 02138

(Received 12 November 2004; accepted 11 March 2005; published online 18 April 2005)

Using analytical modeling and detailed numerical simulations, we investigate properties of hybrid systems of photonic crystal microcavities which incorporate a highly nonlinear ultraSlow light medium. We demonstrate that such systems, while being miniature in size (order wavelength), and integrable, could enable ultrafast nonlinear all-optical switching at ultralow (even single photon) energy levels. © *2005 American Institute of Physics*. [DOI: 10.1063/1.1900956]

For many important applications (e.g., quantum information processing, integrated all-optical signal processing, etc.) it would be highly beneficial to have strong and nearly instantaneous interaction of light with light, preferably happening in a minimal volume. This can be achieved, in principle, by exploiting intrinsic material nonlinearities. Unfortunately, such nonlinearities are fairly weak, so one is forced to make undesirable compromises in interaction time, device-length, and/or power. To optimize the effects, we combine two approaches to enhance optical nonlinearities. One is structural: We design a structure whose geometrical properties enhance the nonlinear interaction; photonic crystals (PhCs), have been proven to be particularly suitable for this purpose.[1] The other approach is to use an ultraslow light (USL) medium with extremely large nonlinear optical response. Nonlinear Kerr coefficients—12 orders of magnitude larger than in AlGaAs—have been measured in such systems.[2] We show how combining these two approaches can lead to all-optical switches of unprecedented characteristics; such switches can be less than λ^3 in size, with switching times faster than 100 ps, and operating at extraordinarily low (even single photon) energy levels. To our knowledge, single-photon nonlinear behavior of cavity-electromagnetically induced transparency has only been discussed qualitatively using generic or heuristic models.[3–5] In contrast, we present results of realistic numerical experiments (including material and radiative losses) on an exemplary system of a PhC microcavity containing a single USL atom. In particular, we perform finite difference time domain (FDTD) simulations with perfectly matched layer boundary conditions,[6] which simulate Maxwell's equations (including dispersion) for such a system exactly (apart for the discretization).

Consider a hybrid PhC microcavity, as shown in Fig. 1: The resonance is confined laterally by index guiding and axially by the one-dimensional PhC gap. We model a two-dimensional (2D) system, since the essential physics is the same as that of its three-dimensional (3D) counterpart, but numerical requirements are now much more tractable. The microcavity in Fig. 1 has only a single resonance that is equally (and weakly) coupled to an input and output waveguide with:

$$T(\omega) \equiv \frac{P_{\mathrm{OUT}}(\omega)}{P_{\mathrm{IN}}(\omega)} = \left| \frac{i\Gamma_{IO}}{\omega - \omega_{\mathrm{RES}} + i(\Gamma_{IO} + \Gamma_{\mathrm{RAD}} + \Gamma_{\mathrm{ABS}})} \right|^2, \quad (1)$$

where P_{OUT} and P_{IN} are outgoing and incoming powers, Γ_{IO}, Γ_{RAD}, and Γ_{ABS} are, respectively, the widths due to coupling to the waveguides, loss from the cavity due to the coupling to the free-space radiation modes, and the intrinsic material absorption, and ω_{RES} is the resonant frequency. The transmission through the cavity is given by the dashed blue curve in Fig. 2, whose width is $\approx \omega_{\mathrm{RES}}/692$. If there were no radiation losses ($\Gamma_{\mathrm{RAD}}=0$), this curve would peak at 100% transmission.

Consider now the insertion of a single USL atom[7] at the center of the microcavity. This could be implemented by using atomic force microscopy techniques, solid-state USL materials,[8] or a single-gas-atom PhC microcavity.[9] The relevant atomic levels of such an atom are shown in Fig. 3(a). In general, one would need to ensure that each of the relevant atomic transitions coincides with an *even* resonant mode of

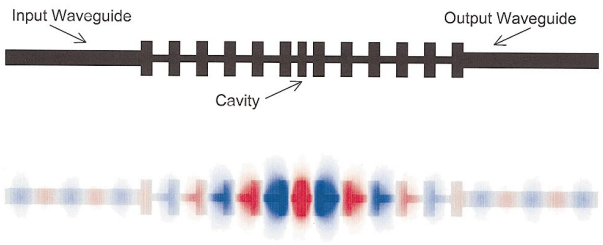

FIG. 1. (Color) PhC microcavity studied in this letter (dielectric profile shown on the top), and the electric field (all pointing out of the plane) of its resonant mode (shown on the bottom, together with the high index material (gray). High index material has $\varepsilon=12$, and is surrounded with air ($\varepsilon=1$). The cavity is implemented by introducing a defect into a periodic structure, of period a. Each periodic cell consists of a thick segment (thickness $1.25a$, length $0.4a$), followed by a thin segment (thickness $0.25a$, length $0.6a$). The defect is introduced by narrowing the length of the central thick element to $0.3a$, and narrowing the length of its two neighboring thin elements to $0.25a$. The incoming and outgoing waveguides have thickness $0.55a$. The runs are performed at a numerical grid resolution of $40pts/a$. Consistency is checked at $20pts/a$, and $80pts/a$.

[a]Electronic mail: marin@alum.mit.edu

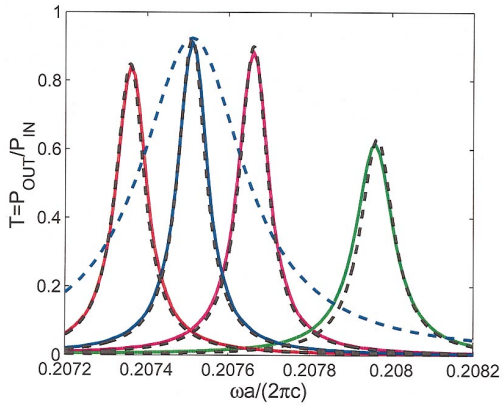

FIG. 2. (Color) Transmission through the system of Fig. 1. The dashed blue curve presents the FDTD calculation when the USL atom is not present. The solid blue curve presents the FDTD calculation with the USL atom present [dispersion given by Fig. 3(b)], and ω_{13} exactly coinciding with the resonance of the cavity without the USL atom present. Red, green, and magenta curves present FDTD calculations when dispersion in Fig. 3(b) is shifted sideways as: Red ($\omega_{13}\rightarrow\omega_{13}*0.999$), magenta ($\omega_{13}\rightarrow\omega_{13}*1.001$), and green ($\omega_{13}\rightarrow\omega_{13}*1.003$). The dashed black curves are predictions of the perturbation theory for their corresponding curves: They are obtained as follows. First, we assume linear dependence of Re$\{\alpha\}$ close to ω_{13}, and quadratic dependence of Im$\{\alpha\}$ close to ω_{13}, with fit parameters obtained from Fig. 3(b); these are needed for Eq. (2). Second, with a series of independent FDTD calculations we obtain a linear fit to Γ_{RAD} in Re$\{\alpha\}$, as required by Eq. (3). Next, we obtain Γ_{IO}, and ω_{RES} from the dashed blue curve above, and calculate V_{MODE} with an independent simulation. Finally, we substitute the expressions obtained by Eqs. (2) and (3) in this manner into Eq. (1), in order to obtain the black dashed curves shown here. As one can see, perturbation theory models the true behavior very faithfully.

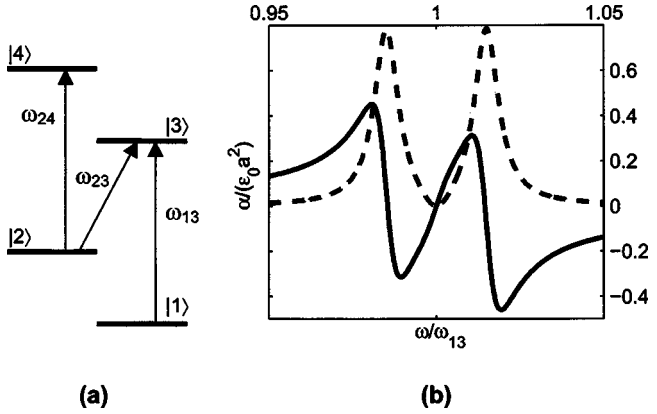

FIG. 3. (a) Schematic of atomic levels in a typical USL system. (b) Normalized polarizability of the USL atom of interest: solid line is Re$\{\alpha\}$, and dashed line is Im$\{\alpha\}$.

the cavity. Next, one would introduce a coupling field at frequency ω_{23} into the cavity, in order to establish USL for the probe frequencies ω which are close to the ω_{13} transition. The polarizability of a typical USL atom is shown in Fig. 3(b).

Introduction of a highly dispersive polarizable object into a cavity has two important effects. First, it changes the resonant frequency of the cavity. According to perturbation theory:[1]

$$\tilde{\omega}_{\mathrm{RES}} \approx \omega_{\mathrm{RES}}\left[1-\frac{\alpha}{2\epsilon V_{\mathrm{MODE}}}\right], \tag{2}$$

where the induced dipole moment $\mathbf{p}=\alpha\mathbf{E}$ (here, $\mathbf{E}$ is the electric field at the position of the dipole, and α is the atomic polarizability), $V_{\mathrm{MODE}}\equiv(\int_{\mathrm{MODE}}d^3x\epsilon|\mathbf{E}|^2)/\epsilon|\mathbf{E}_{\mathrm{MAX}}|^2$ is the modal volume, and ϵ is the dielectric constant of the host medium. Note that since α is in general complex, Eq. (2) also causes an effective change in Γ_{ABS} as: $\tilde{\Gamma}_{\mathrm{ABS}}\approx\Gamma_{\mathrm{ABS}}+\omega_{\mathrm{RES}}\mathrm{Im}\{\alpha\}/2\epsilon V_{\mathrm{MODE}}$. Second, this object results in a change of geometry of the cavity, thereby modifying its coupling to the free-space radiation modes (Γ_{RAD}). Usually, power scattered by an induced dipole is $\propto|\mathbf{p}|^2$. However, in our case, both the induced dipole, and the cavity mode itself scatter out of the cavity a significant portion of power into the same single mode (dipole far-field radiation expansion). Consequently, their fields (rather than powers) add, and the change in the radiated power ΔP_{RAD} has a component linear in $\mathbf{p}$. Since Re$\{\alpha\}\gg$Im$\{\alpha\}$ for a typical USL application:

$$\Gamma_{\mathrm{RAD}} \approx \Gamma_{\mathrm{RAD}}(\mathbf{p}=0)+\xi\,\mathrm{Re}\{\alpha\}+\ldots \tag{3}$$

where ξ is determined by the geometry of the cavity, and has to be calculated for each cavity separately: One simulates systems with a few different values of α, and fits Γ_{RAD} to a straight line. For our 2D cavity from Fig. 1, we calculate $\xi\approx 0.0012c/(a^3\epsilon_0)$.

The enormous dispersive behavior,[2] like the one shown in Fig. 3(b), drastically narrows the transmission resonance width of the cavity for probe frequencies ω close to ω_{13}.[10] Intuitively, the large dispersion implies low group velocity, so each "bounce" between the two mirrors of the cavity takes a longer time, meaning that the light spends a longer time in the cavity. For the particular case of the dipole shown in Fig. 3(b), the FDTD calculation of narrowing gives a factor of $\approx$3.3,[11] as shown by the solid blue line in Fig. 2. Finally, we introduce an additional (control) field into the cavity, with a frequency close to ω_{24}, in order to perform the switching of the probe field ω.[12,13] The control field causes a Stark shift of level $|2\rangle$, sliding the whole dispersion curve in Fig. 3(b) sideways. This switching behavior is displayed by red, green, and magenta curves in Fig. 2.

We can now use the analytical model[14] to understand the behavior of such devices in various USL parameter regimes. We start by writing the expression for α of an USL atom, for ω close to ω_{13} using arguments similar to those of Ref. 15:

$$\alpha \approx \frac{6e^2 f_{13}}{m_e\omega_{13}}\left[\frac{\Delta_P}{|\Omega_C|^2}+2i\Gamma_3\left(\frac{\Delta_P}{|\Omega_C|^2}\right)^2\right], \tag{4}$$

where f_{13} is the oscillator strength of $|3\rangle\rightarrow|1\rangle$ transition, Γ_3 is the decay width of state $|3\rangle$ (which can, in general, be different than the free-space decay width of state $|3\rangle$: In our case, it is larger by a factor $\sim Q\lambda^3/V_{\mathrm{MODE}}$ [Q being the quality factor due to cavity-QED (quantum electrodynamics) effects], Ω_C is the Rabi frequency of the coupling field (at frequency ω_{23}), and $\Delta_P\equiv\omega-(\omega_{13}-|\Omega_{24}|^2/4\Delta\tilde{\omega}_{24})$, where Ω_{24} is the Rabi frequency of the control field, $\Delta\tilde{\omega}_{24}=\Delta\omega_{24}-i\gamma_{24}$, $\Delta\omega_{24}$ is the difference in frequencies between the control field, and ω_{24}, while γ_{24} is the decay width of the $|4\rangle\rightarrow|2\rangle$ transition. For the application of interest, we can approximate: $\Delta\tilde{\omega}_{24}\approx\Delta\omega_{24}$. We substitute Eqs. (2)–(4), into Eq. (1) to obtain:

$$T(\omega)=\left|\frac{i\Gamma_{IO}}{\omega-\omega_{\mathrm{RES}}+\frac{c}{v_G}\Delta_P+i\left[\Gamma_{\mathrm{RAD}}(\mathbf{p}=0)+\xi\frac{6e^2f_{13}}{m_e\omega_{13}}\frac{\Delta_P}{|\Omega_C|^2}+\Gamma_{IO}+\frac{6e^2f_{13}\Gamma_3}{V_{\mathrm{MODE}}\epsilon m_e}\left(\frac{\Delta_P}{|\Omega_C|^2}\right)^2\right]}\right|^2, \tag{5}$$

where we define: $3e^2f_{13}/m_eV_{\mathrm{MODE}}\epsilon|\Omega_C|^2\equiv c/v_G$; v_G has a simple physical interpretation: It is the group velocity of propagation in uniform USL media, consisting of (same) USL atoms, but with atomic density $1/V_{\mathrm{MODE}}$.

In regimes of strong USL effects, $c/v_G\gg 1$, so the real part of the denominator of Eq. (6) can be approximated as $\omega-\omega_{\mathrm{RES}}+c/v_G\Delta_P\approx c/v_G\Delta_P$, so $T(\Delta_P=0)\approx\Gamma_{IO}^2/[\Gamma_{IO}+\Gamma_{\mathrm{RAD}}(\mathbf{p}=0)]^2$, which is the same as the peak transmission of the cavity without the USL atom. Furthermore, for properly designed microcavities, and properly implemented USLs, absorption [term proportional to Γ_3 in Eq. (5)], and changes to the cavity geometry [term proportional to ξ in Eq. (5)] can both be neglected. Thus, the width of the transmission curve [Eq. (5)] is given by $\approx[\Gamma_{IO}+\Gamma_{\mathrm{RAD}}(\mathbf{p}=0)](v_G/c)$, so the narrowing factor is $\approx v_G/c$. To obtain switching, we need to shift the resonance by more than its width:

$$\frac{c}{v_G}\frac{|\Omega_{24}|^2}{4|\Delta\tilde{\omega}_{24}|}>\Gamma_{\mathrm{RAD}}(\mathbf{p}=0)+\Gamma_{IO}. \tag{6}$$

The optimal efficiency of our systems is apparent from Eq. (6). The right-hand side of the equation is the transmission width of the cavity without the USL atom present: The larger its Q, the more efficient the system. The left-hand side is just the Kerr-effect induced change in the resonant frequency of the cavity. The strength of this Kerr-effect is greatly enhanced because of three factors: (c/v_G) can be made large, $\Delta\tilde{\omega}_{24}$ can be made small (so we are exploring nonlinearities close to the resonance which one cannot do in usual nonlinear systems because of huge absorption), and for a given incoming power P_{24}, the cavity enhancement effects and the small modal volume both make Ω_{24} large.

Before concluding, we estimate quantitative performance characteristics of a 3D device of the type we describe. First, we assume that the modal extent in the direction out of the page in Fig. 1 is roughly the same as the modal extent in the direction perpendicular to the waveguide in the plane of the figure. This gives an estimate of $V_{\mathrm{MODE}}\approx 0.009\lambda_{\mathrm{RES}}^3$. As an example, we will use a resonance of the sodium atom with $\lambda_{\mathrm{RES}}=589$ nm. We assume a resonance-narrowing factor due to USL of $c/v_G\approx 30$, leading to a transmission width (and hence the available operational bandwidth in ω) $\delta f\approx 25$ GHz. (For comparison, if we chose to use the experimental parameters of Ref. 2, the narrowing factor would be $>10^7$!) To implement switching, the induced Stark shift is: $|\Omega_{24}|^2/(4|\Delta\omega_{24}|)>2\pi*\delta f\approx 2\pi*25$ GHz.[7] So, if we take $\Delta\omega_{24}=60$ GHz (which would provide us with ~10 GHz operational bandwidth for the control field), the needed intensity of the control field in air (for sodium) would be $I_{24}\approx 50\ \mathrm{GW/m^2}$,[2] while the field inside the cavity is: $|\mathbf{E}_{24}|^2=2I_{24}/(c\epsilon_0)$. The needed input power $P_{24}=\omega_{\mathrm{RES}}U_{24}/(2Q_{24})=(\epsilon\pi V_{\mathrm{MODE}}I_{24})/(\epsilon_0\lambda_{\mathrm{RES}}Q_{24})$, where U_{24} is the control field's modal energy, and $Q_{24}\approx 692$ is its transmission Q for the cavity of Fig. 1. We conclude that $P_{24}\approx 8.5\ \mu$W. With similar reasoning, we can show that the power in the coupling field needs to be $P_C\approx 20\ \mu$W. Finally, the number of the control-field photons needed to be present in the cavity in order to induce the switching is $N_{24}=V_{\mathrm{MODE}}\epsilon|\mathbf{E}_{24}|^2/2\hbar\omega_{24}\approx 11$. Each of these photons spends $\sim Q_{24}/\omega_{24}\sim 0.22$ ps in the cavity, while the switching time is $\sim\pi/\Delta\omega_{24}\sim 52$ ps; so the switching is performed by a total of $N_{24}\sim 2600$ photons. By exploring even more extreme regimes of USL parameters and/or higher-Q PhC cavities, one can easily reach the single-photon optical nonlinearity operation regime, which has been elusive thus far.

This work was supported in part by DARPA Research Contract No. FA8750-04-1-0134.

[1] M. Soljacic and J. D. Joannopoulos, Nat. Mater. **3**, 211 (2004).
[2] L. V. Hau, S. E. Harris, Z. Dutton, and C. H. Behroozi, Nature (London) **397**, 594 (1999).
[3] A. Imamoglu, H. Schmidt, G. Woods, and M. Deutsch, Phys. Rev. Lett. **79**, 1467 (1997).
[4] S. Rebic, S. M. Tan, A. S. Parkins, and D. F. Walls, J. Opt. B: Quantum Semiclassical Opt. **1**, 490 (1999).
[5] M. J. Werner and A. Imamoglu, Phys. Rev. A **61**, 011801(R) (1999).
[6] For a review, see A. Taflove, *Computational Electrodynamics: The Finite-Difference Time-Domain Method* (Artech House, Norwood, Mass., 1995).
[7] Since there is only one atom, the Doppler broadening in gaseous USL systems, or the inhomogeneous broadening in solid-state systems (e.g., 5GHz in Pr:YSO) due to the host is not an issue anymore, while the remaining uncertainty in the exact level positions can be much smaller than the cavity resonance width.
[8] A. V. Turukhin, V. S. Sudarshanam, M. S. Shahriar, J. A. Musser, B. S. Ham, and P. R. Hemmer, Phys. Rev. Lett. **88**, 023602 (2002).
[9] J. Vuckovic, M. Loncar, H. Mabuchi, and A. Scherer, Phys. Rev. E **65**, 016608 (2001).
[10] M. Soljacic, E. Lidorikis, L. V. Hau, and J. D. Joannopoulos, Phys. Rev. E **71**, 026602 (2005).
[11] In our numerics, we model the USL atom as a small-area object ($2.4\times 10^{-4}\lambda_{\mathrm{RES}}^2$), with large highly-dispersive susceptibility. The required dispersion shape is obtained with two absorption lines sandwiching a gain line; such a shape closely resembles a typical USL dispersion.
[12] H. Schmidt and A. Imamoglu, Opt. Lett. **21**, 1936 (1996).
[13] S. E. Harris and L. Hau, Phys. Rev. Lett. **82**, 4611 (1999).
[14] The fairly broad-bandwidth of our pulses of interest masks influence of the atom-cavity coupling effects on the resonant frequencies; thus, a semiclassical analysis is appropriate.
[15] Z. Dutton, Ph. D. thesis, Harvard University, 2002.